ARCTIC & ANTARCTIC SEA ICE CONCENTRATION AND ARCTIC SEA ICE DRIFT ESTIMATED FROM SPECIAL SENSOR MICROWAVE DATA

USER'S MANUAL

Version 2.1, February 2007

Robert Ezraty, Fanny Girard-Ardhuin, Jean-François Piollé

Laboratoire d'Océanographie Spatiale
Département d'Océanographie Physique et Spatiale
IFREMER, Brest, France

Lars Kaleschke and Georg Heygster

Institute of Environmental Physics
University of Bremen, Germany

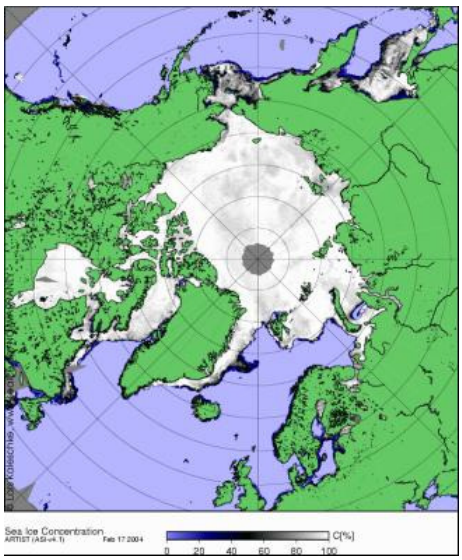

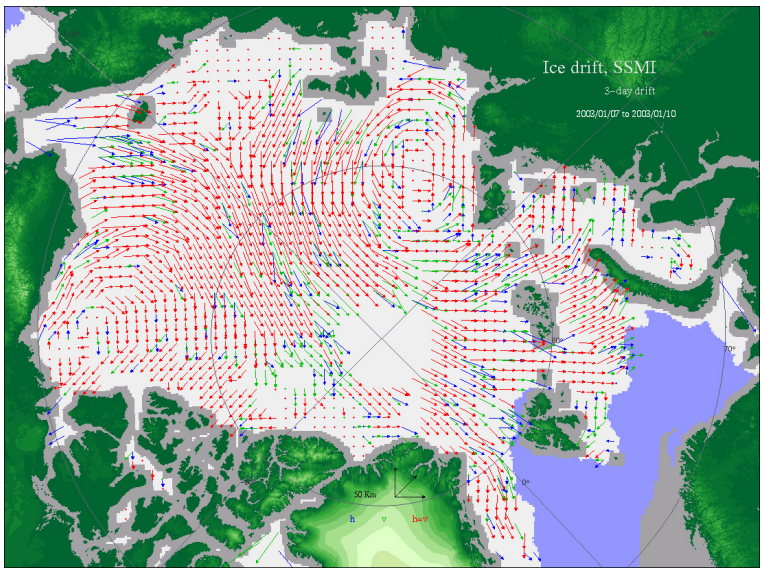

Universität Bremen

ERSAT
French Processing and Archiving Facility

Ifremer

Acknowledgments

The Sea Ice drift project was initiated by Alain Cavanié when he was IFREMER Senior Scientist at Département d'Océanographie Physique et Spatiale/Laboratoire d'Océanographie Spatiale. He explored, the many 'bits and pieces' which paved the way to the operational algorithm presently in use at IFREMER/CERSAT.

The National Snow and Ice Data Center (NSIDC) provides the gridded Special Sensor Microwave Imager brightness temperature data and the Physical Oceanographic Data Active Archiving Center (PODAAC) provides the L2A level QuikSCAT backscatter data.

The in-situ drifting buoys data set used for validation was extracted from the International Arctic Buoy Program (IABP) archive.

The ASI algorithm has been developed in the framework of the EU-funded project ARTIST (ENV4-CT97-0497-0487).

Our thanks to each of these contributors.

Contents

Revision history

Version	Name	Date	Comments
V0 draft	Ezraty	15/02/2004	
V0.1	Piollé	01/03/2004	Section 3 added
	Ezraty	03/03/2004	Lars inputs added
V1.0	Ezraty	01/04/2004	Flag table in 3.1.1. updated
V2.0	Girard-Ardhuin	10/02/2006	Upgrade incomplete daily dataset New quicklooks New data access Introduction of coastlines data Monthly concentration maps
V2.0	Girard-Ardhuin	20/04/2006	New quicklooks path
V2.0	Girard-Ardhuin	12/05/2006	Concentration grid information added Section 2.3 added
V2.1	Girard-Ardhuin	02/02/2007	Upgrade incomplete daily dataset New coastlines data correction New quicklooks New data access Antarctic concentration added Climatology added

Background / Introduction

The Special Sensor Microwave Imager (SSM/I) brightness temperatures have been widely and regularly used since 1987 to estimate sea ice extent and sea ice concentration. More recently, SSM/I derived sea ice drift in Arctic and Antarctic have been obtained, for example by Liu *et al.*(1998). All these products provide an ocean-scale view of the sea ice dynamic.

The development of applications of scatterometry over sea ice, since the early 1990's, has recently lead to a sea-ice drift product (Ezraty *et al.*, 2007a). This data set is built from the daily QuikSCAT scatterometer backscatter maps and produced at IFREMER on a 12.5 km x 12.5 km grid (Ezraty and Piollé, 2001). In order to compare the QuikSCAT derived drifts to those of the SSM/I, the drift algorithm used was applied to the SSM/I 85GHz brightness temperatures maps. Not only, the match between the two data set was found very good (Carlut, 2003) in the common area surveyed by both sensors but it was also shown that: First, because of its sensor geometry, QuikSCAT provides drift data in the large "blind" zone of the SSM/I around the North Pole and Second, because of the backscatter properties of the sea ice surface, significant more drift information was available earlier in Autumn and later in Spring than with the SSM/I. Furthermore, it was shown that both drift data sets are complementary in that the number of drift vectors of the merged drift map is increased by 12 to 15% compared to the QuikSCAT derived drift map (Ezraty *et al.*, 2007b). This improvement is a real asset since it decreases, by the same amount, the number of interpolations which might be required for example either to " follow", as a function of time, any sea-ice element or to use a consistent number of drift vectors for climatological and/or statistical purposes at prescribed grid-nodes or to built up an interpolated drift vector map adapted to the modeller's specific requirements.

The merged sea ice drift data product is now operational and distributed. Since the 12.5 km x 12.5 km resolution sea ice concentration maps and the SSM/I derived drift data are computed as part of the processing, it was decided to make them available to users.

This report is composed of three sections. The 12.5 km x 12.5 km resolution sea ice concentration product is presented in Section 1 with short references to the ASI algorithm and the brightness temperatures data sets. Section 2 deals with the SSM/I drift algorithm, mainly with the pre-processing of the 85 GHz Tb required to apply the drift algorithm. The data access, data structure and data formats are described in Section 3.

1. The sea ice concentration data

Daily brightness temperatures and ice concentration maps as well as weekly and monthly averages are already available. For example, the National Snow and Ice Data Center (NSIDC), Boulder, Colorado distributes, daily, through its web site (http://nsidc.org) both the low frequency brightness temperature (19V, 19H, 22V, 37H and 37V GHz) with a resolution of 25 km x 25 km and the high frequency (85H and 85V GHz) brightness temperature on a higher resolution map (12.5 km x 12.5 km).
Among other possible algorithms, sea ice concentration is usually estimated either from the NASA Team Algorithm, NTA, (Cavalieri *et al.,* 1992) or from the Bootstrap algorithm (Comiso *et al.*, 1997). Both algorithms use the low frequency channels, yielding the 25 km x 25 km resolution of the sea ice concentration maps distributed by the NSIDC.

1.1 The ASI algorithm

The need for higher resolution sea ice concentration data to monitor the marginal ice zones, polynya and leads opening required new algorithms relying on the 85 GHz brightness temperatures. Among these algorithms, the Artist Sea ice (ASI) algorithm developed at the University of Bremen, tested and validated for various situations, provided reliable results (Kaleschke *et al*., 2001). Most of the following is extracted from this reference. For more details on the ASI algorithm see also, Kern *et al.*, 2003 and Kaleschke, 2003.

The ASI algorithm is an hybrid model which combines the Svendsen algorithm (Svendsen *et al.*, 1987) for ice covered areas and the NASA Team Algorithm for the ice-free ocean. The Svendsen Algorithm (SVA) builds on a radiative transfer equation linking the polarization difference, $P = Tb_{85v} - Tb_{85h}$ to ice concentration, C, physical temperatures of water and ice, atmospheric optical depth and the difference of emissivity at V and H pol. of water and ice (figure 1).

The basic assumption of the SVA is that the atmospheric influence can be represented by a smooth function as: $C = \sum_{i=0}^{i=3} d_i P^i$. The low resolution NASA Team ice concentration are used to constraint the determination of the d_i's via the selection of the ice and water tie points (P0 and P1).

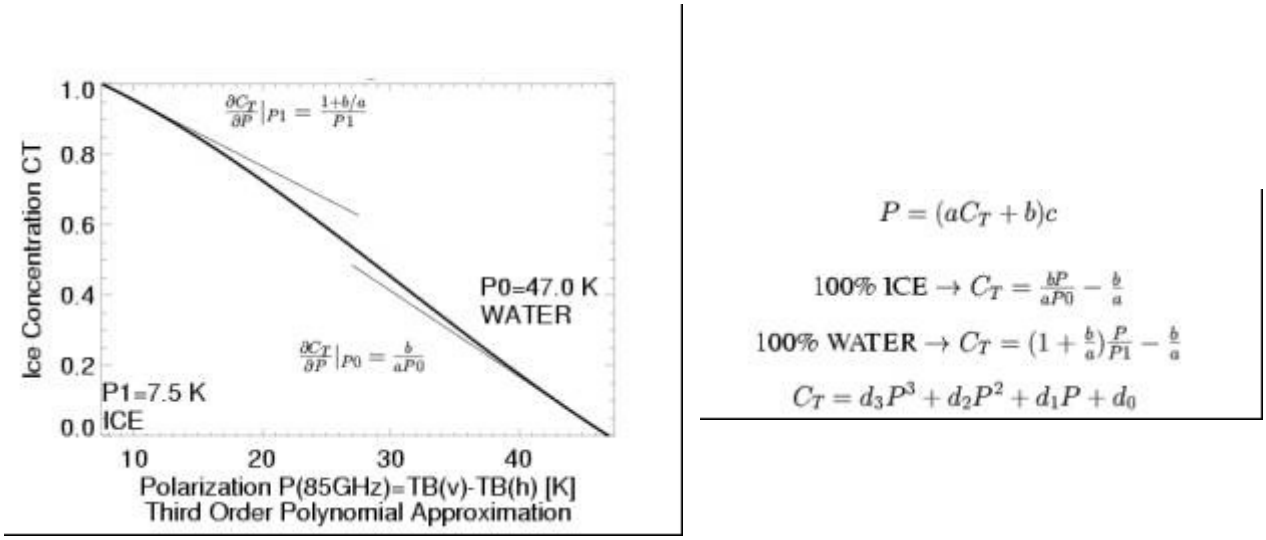

Figure 1 : Sketch of the ASI algorithm

A weather filter is applied, as part of the NTA algorithm, to dismiss spurious ice concentration values (Cavalieri *et al*., 1995).

The original ASI sea ice concentration maps can be browsed at http://www.seaice.de. The archive starts on January 1st, 1996.

1.2 Implementation of the ASI algorithm

The ASI source code was provided to IFREMER by IUP-Bremen (Lars Kaleschke) and implemented as part of the SSM/I drift processing.

The Arctic & Antarctic concentration grids at 12.5 km resolution are presented in figure 2. These are polar stereographic projections, the projection plane is tangent to the earth at 70°N latitude so that little or no distortion would occur in the ice zone.
A program which links geographic location (latitude, longitude values) to *i,j* indexes of the NSIDC grid is available (see Section 6.3 in Ezraty *et al*., 2007a); another solution is to have the complete grid coordinates (latitude, longitude) which can be found at
ftp://ftp.ifremer.fr/ifremer/cersat/products/gridded/psi-concentration/data/arctic/grid_north_12km.nc.gz
ftp://ftp.ifremer.fr/ifremer/cersat/products/gridded/psi-concentration/data/antarctic/grid_south_12km.nc.gz

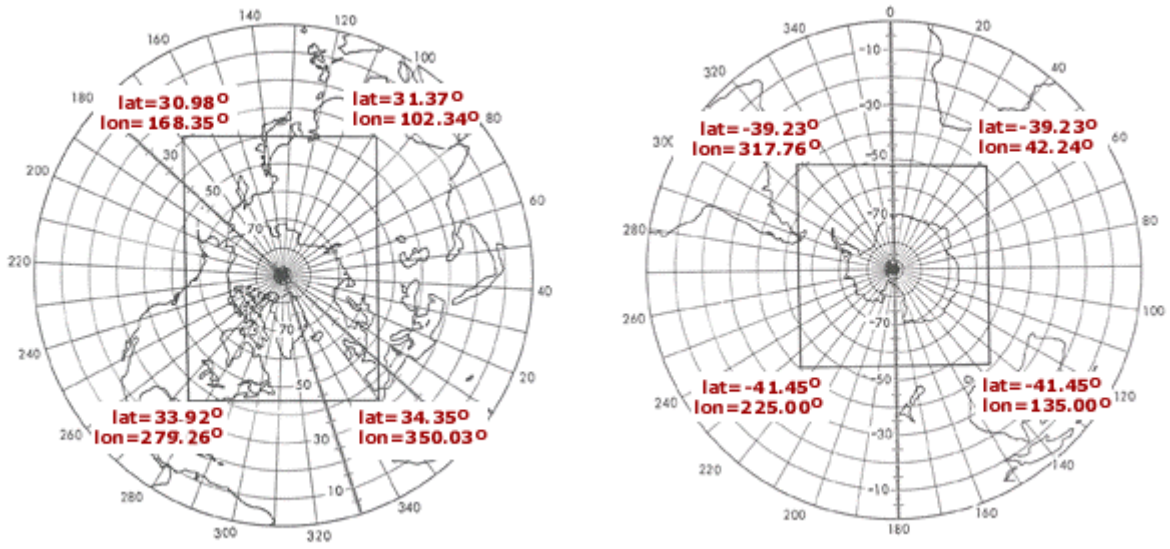

Figure 2 : Maps of sea ice concentration grid spatial coverage in Arctic (left) and Antarctic (right). From NSIDC documentation.

1.2.1 Specific adjustments

Two minor modifications have been performed on the final concentration data:

- The IFREMER monthly-varying climatological sea ice mask is applied to erase the spurious ice areas at low latitudes (figure 3).

These sea ice artefacts occur because of the sensitivity of the 85 GHz channels to weather influence (storm conditions). They can be easily identified, visually, using a time series of concentration maps. Erasing automatically these spurious concentration data in likely sea ice areas is much more difficult unless restrictive conditions are employed. A typical constraint is to allow ice to grow /retreat only as attached to the main ice pack. This does not solve the cases when ice artefacts are located at the ice/water limit or the cases when new-ice patches grow locally in the open sea. Such a processing is not applied here. The main reason is that, in the drift algorithm, the correlation between the "polluted" patterns of the time lagged maps drops dramatically as the storm moves away. By the way, this numerical technique cannot be applied to erase the sea-ice artefacts at the ice/water interface because it destroys the resolution enhancement provided by the ASI algorithm.

- Land contamination effects exist, concentrations are computed on a three pixel-wide band along the coast lines but are certainly quantitatively not reliable (see quality flags in Section 3.1.1), a correction has been applied to delete some of the unrealistic concentrations in this area. In the drift processing, a three pixel-wide band along the systematic discontinuities is neutralized (Ezraty *et al.*, 2007a).

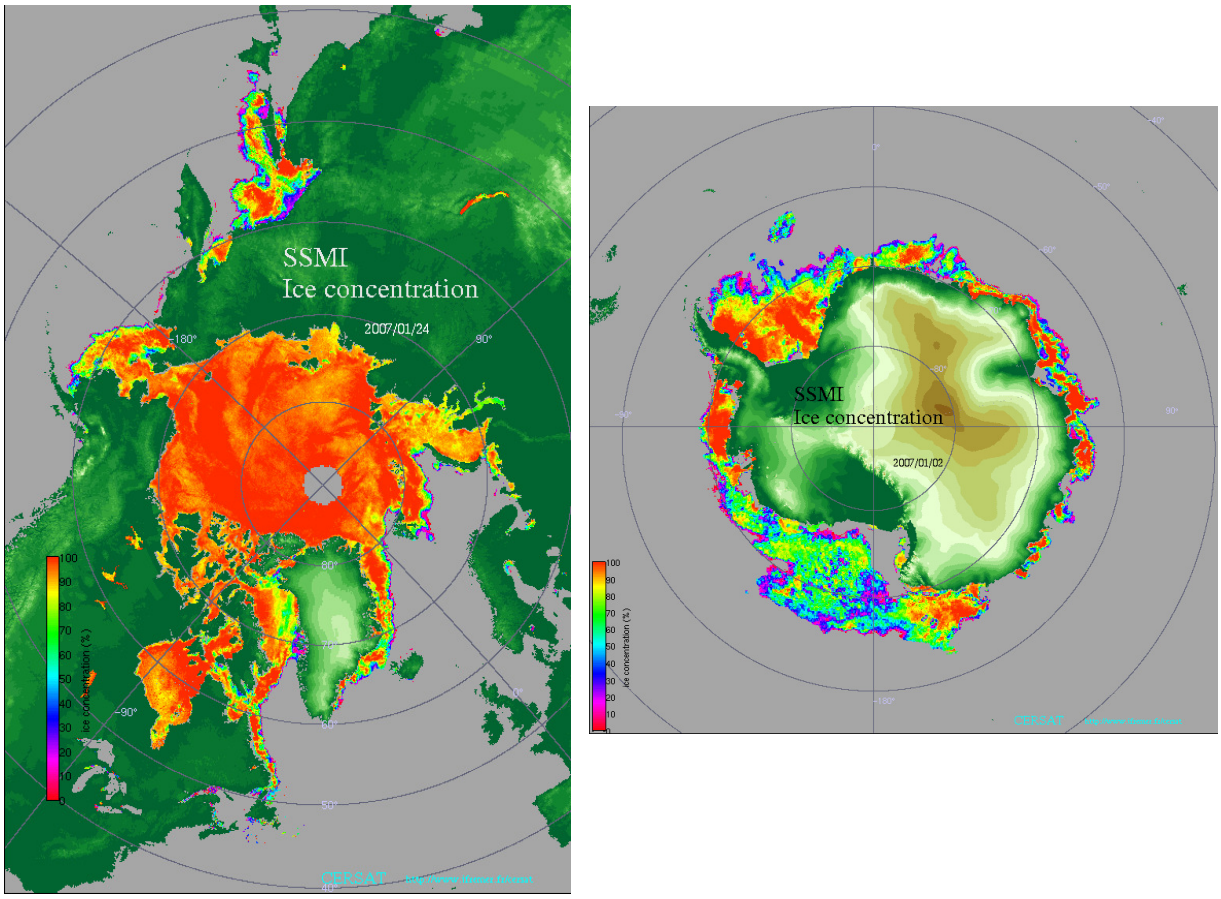

Figure 3 : Examples of Arctic (left) and Antarctic (right) sea ice concentration maps.

1.2.2 The SSM/I brightness temperatures data set

The systematic processing of SSM/I brightness temperature data started, at IFREMER, in February 2004, targeting the production of a merged QuikSCAT-SSM/I drift data set since the beginning of the QuikSCAT mission (July 1999).

The brightness temperature archive for winter 1999-2000 until winter 2002-2003 from the CDRoms distributed by the NSIDC. A "winter" period spans from September 1st on year N until May 31st on year N+1. Since September 1st, 2003, the brightness temperatures are downloaded, daily, from the Near Real Time archive of NSIDC at
ftp://sidads.colorado.edu/pub/DATASETS/PASSIVE_MICROWAVE/POLAR_STEREO/DATA/TB/F13/NEAR_REAL_TIME/

2. The SSM/I derived sea ice drift products

The core, the validation part and the output file of the drift algorithm applied to each of the SSM/I Tb's 85 GHz channels are absolutely identical to that of the QuikSCAT composite backscatter map. These steps are described in Ezraty *et al.* (2007a) and will not be repeated here. Of course, the brightness temperatures and the QuikSCAT backscatter values being mapped on the same 12.5 km x 12.5 km grid, the drift-grid (62.5 km x 62.5 km) is also identical and covers the same geographic area.

The main difference is the pre-processing of the Tb-maps, in order to prepare for the computation of the field of Laplacian which is the starting step of the drift algorithm itself. In order to built a self consistent SSM/I product, the ice edge is taken from the sea-ice concentration maps described in Section 1.

2.1 The pre-processing of the brightness temperature maps

The major problem of the brightness temperature maps is the wide "blind-area" around the North Pole. This circular area has a radius of about 254 km, which compares to that of the QuikSCAT inner beam (230 km), while that of QuikSCAT outer beam is an order of magnitude smaller (40 km). Such a permanent data discontinuity will be enhanced by the double spatial derivative performed at the first step of the drift algorithm and will induce a 'strange attractor' effect when estimating the drift vector via the correlation between the lagged Laplacian fields. To overcome this effect, the blind-area is assimilated to a land area, adjusted daily to each map, and expanded by a three pixel-wide band to account for the median filter applied (Ezraty *et al.*, 2007a).

Each 85 GHz brightness temperature map is treated separately, since the polarization reveals different structures of the sea ice field. Using a combination of these two maps would bluer the spatial structure to be detected. It follows that no noise reduction on the input brightness temperature maps can be performed as it is done for the QuikSCAT backscatter maps.

2.2 The SSM/I derived drift maps

During the freeze-up period (September to mid-October), given the variability of the radiative properties of the sea ice layer, less than 50% of the possible drift-vectors can be determined. Its only by mid-October that this level rises to 70%. Due to surface temperature changes and because of the modifications due to precipitations, large fluctuations (by more than 10%) of this level occur until early spring. As soon as surface melting and ponding occur, the level drops down to less than 50% by late April.

Figure 4 presents a typical winter-time drift map where identical drift-vectors obtained from each SSM/I channels are in red, V polarization channel vectors are displayed in green and H polarization channels are in blue. Globally, all other the winter period, the V polarization channel provided more vectors than the H polarization channel.

It can be observed that, at some locations (for example in the Chukchi Sea) , the drift vector retrieved from the two channels do not match. The sum of the differences on each components seldom exceed three pixels. These differences are attributed partly to the noise level of each pixel of the temperature maps and mainly to the different signature of the sea ice cover with polarization (for example with concentration).

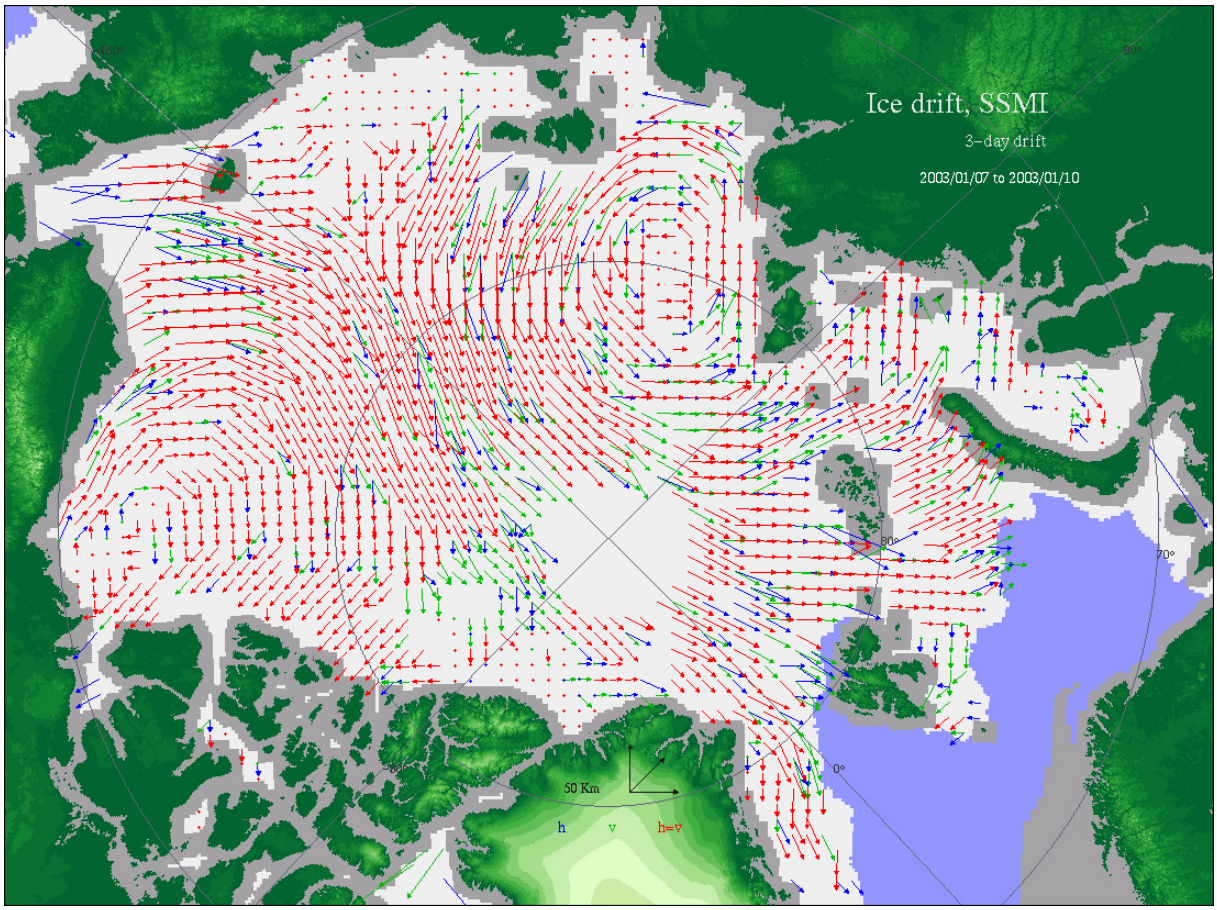

Figure 4 : Drift vectors at 3-day lag computed from SSM/I 85 GHz brightness temperature maps (January 7th-10th 2003). Identical drift for H and V channel, V channel, H channel. Drift vectors less than one pixel are marked with a cross.

2.3 More drift products

Other drift products exist at CERSAT-IFREMER :

- QuikSCAT drift (see Ezraty *et al*. ,2007a)
- Merged drift (SSM/I combined with QuikSCAT) (see Ezraty *et al*., 2007b)
- AMSR-E drift (see Ezraty *et al*., 2007c)

3. Data access & organization

3.1 Sea-ice concentration

3.1.1. Data

Sea ice concentration daily and monthly maps are estimated all year long. A 15-year monthly climatology is also available (1992-2006). The datasets are available at the following ftp address ftp://ftp.ifremer.fr/ifremer/cersat/products/gridded/psi-concentration/data/

The *psi-concentration* folder contains the sea-ice concentration data, documentation and quicklooks. It is organized as follow :

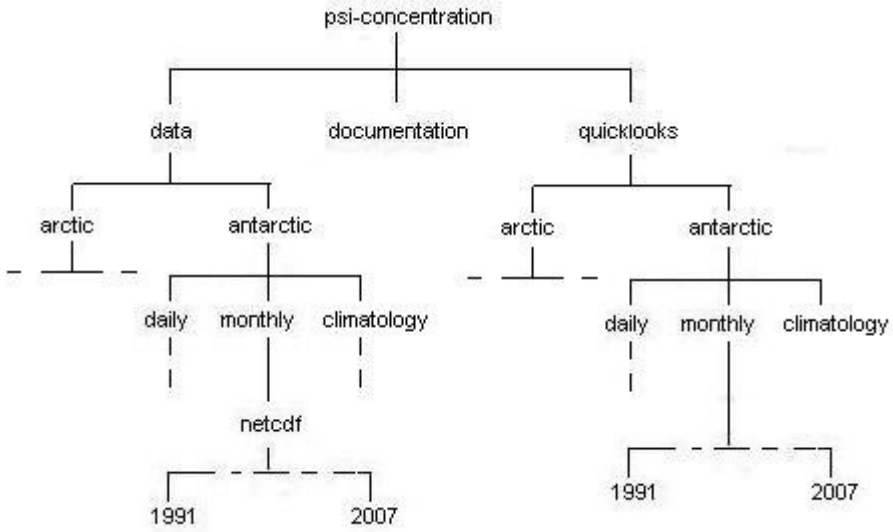

Monthly concentrations are estimated from the daily concentrations data. A mean concentration value, at each pixel, is considered as significant of sea ice occurrence if sea ice is present for more than 20 days during the month.
Monthly climatology concentrations are estimated from the monthly concentrations data, the median is calculated.
Each concentration map is mapped over the NSIDC 12.5 km x 12.5 km grid (see Section 1.2).

The data are stored in NetCDF format (see Section 3.2.1). The NetCDF format is self-explanatory and contains the variable names, scaling factors and units. A quality flag is provided in addition to the concentration map, it is a two field byte. The significance of each bit is as follow.

Daily concentration

bit	description
0	Land pixel
1	Bad pixel
2	Three pixel wide neutral zone (*see Section 1.2.1*), the concentration is computed although the sea ice temperature data are land contaminated
3	Open ocean, Ifremer mask (*see Section 1.2.1*)
4-7	spare

Monthly concentration

bit	description
0-4	Number of days when ice is present within the pixel area (maximum = 31)
5	Land
6	No data
7	Three pixel wide neutral zone (*Cf. Section 1.2.1*), the concentration is computed although the sea ice temperature data are land contaminated

Monthly climatology concentration

bit	description
0-4	Number of years when ice is present within the pixel area for the selected month (maximum = 15)
5	Land
6	No data
7	Three pixel wide neutral zone (*Cf. Section 1.2.1*), the concentration is computed although the sea ice temperature data are land contaminated

Unavailable brightness temperature maps induce data gaps in the time series of daily concentration maps. The distinction is done between unavailable data (m : missing) and partial-coverage data (c) (*see Annex*).

3.1.2 Quicklooks

Daily and monthly concentration quicklook pictures (example in figure 3) are available at
ftp://ftp.ifremer.fr/ifremer/cersat/products/gridded/psi-concentration/quicklooks/

3.2 Sea ice drift

Ice motion is estimated during typical winter periods which starts on October 1st, and ends on April 30th, the following year. Depending on the winter period considered, daily drift estimates can be computed a few days prior or after these dates. These data are not included in the present product in order to maintain the data set homogeneity but they are available on request.

The data set is available at the following ftp address

ftp://ftp.ifremer.fr/ifremer/cersat/products/gridded/psi-drift/data/arctic/intermediate/ssmi-h/
for H polarization and

ftp://ftp.ifremer.fr/ifremer/cersat/products/gridded/psi-drift/data/arctic/intermediate/ssmi-v/
for V polarization

The psi-drift folder contains the sea-ice drift motion vectors, documentation and quicklooks. It is organized as follow (there is one distinct folder for each SSM/I polarization) :

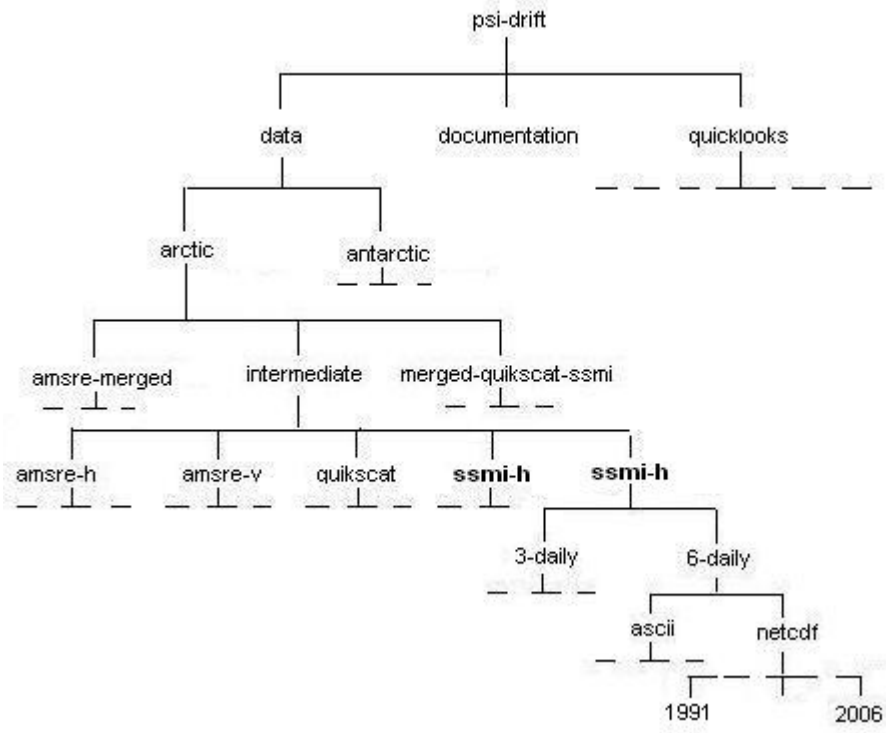

3.2.1. Data

The sea-ice drift vectors are computed over 3 days and 6 days respectively. The data are stored in two different formats.

ASCII format

Each file, contains the list of all retrieved vectors. Columns corresponds to the following parameters : <vector index>, <latitude of start point>, <longitude of start point>, <latitude of end point>, <longitude of end point>, <quality flag>.
The vector index starts with a value of 0.
The quality flag values are : -4, -3, -2,-1, 1 or 6. Negative and zero values correspond to No displacement estimated or NON validated displacements.

NetCDF format

Each vector (given by its origin latitude-longitude location, zonal and meridional components, and its quality flag) is mapped over the NSIDC grid. The grid is stored in a NetCDF file. Detailed information on this format is available at http://www.unidata.ucar.edu/packages/netcdf/

The NetCDF format is self-explanatory and contains the variable names, scaling factors and units. Quality flag values are in signed byte. It follows that the negative values (-1, -2, -3 and –4) may be read as (2^8 + quality flag) depending on the reading software.

Quality flag

The meaning of the quality flag is defined as follow :

value	validity	description
6	OK	At least one component of the drift vector > 5 pixels
1		All tests passed
0	Not OK	No correlation estimated (land or boundaries)
-1		ECMWF wind field test failed
-2		Local spatial coherence not valid (mean+4 standard deviations)
-3		Local spatial coherence not valid (median +2 standard deviation)
-4		Maximum lagged correlation < 0.6

3.2.2 Quicklooks

Quicklook pictures of SSM/I drifts (example in figure 4) are available at
ftp://ftp.ifremer.fr/ifremer/cersat/products/gridded/psi-drift/quicklooks/arctic/intermediate/ssmi/

References

Carlut C., Validation critique et fusion de champs de dérives des glaces de mer en Arctique. Rapport de projet de fin d'études. Rapport IFREMER/DRO/LOS 2003/03. (*in French*). 2003

Cavalieri, D. J., Sea ice algorithm, in *NASA Sea ice validation program for the Defense Meteorological Satellite Program Special Microwave Imager: Final report*, 95 pp., NASA Technical memorandum 104559, National Aeronautics and Space Administration, Washington, DC, 1992.

Cavalieri, D. J., K. M. St. Germain, and C. T. Swift. Reduction of weather effects in the calculation of sea-ice concentration with DMSP SSM/I. *J. Glaciology*, 41(139):455-464, 1995.

Comiso, J.C., D. Cavalieri, C. Parkinson, and P. Gloersen, Passive microwave algorithms for sea ice concentrations, *Remote Sensing of Environment*, 60,357-384, 1997

DMSP SSM/I Brightness temperature grids for the polar regions on CD-ROM, 1990, User's Guide. National Snow and Ice Data Center, Boulder, Colorado, U.S.A.

Ezraty R. and J. F. Piollé, SeaWinds on QuikSCAT Polar Sea Ice Grids, User Manual. CONVECTION report N° 5, V1.1, August 2001. Greenland Sea Convection Mechanism and Their Implications, Fifth Framework Programme of the European Commission 1998-2002, Contract N° EVK2-2000-00058.

Ezraty R., F. Girard-Ardhuin and J. F. Piollé, Sea-ice drift in the Central Arctic estimated from SeaWinds/QuikSCAT backscatter maps. User's Manual, Version 2.2, February 2007a.
ftp://ftp.ifremer.fr/ifremer/cersat/products/gridded/psi-drift/documentation/quikscat.pdf

Ezraty R., F. Girard-Ardhuin and J. F. Piollé, Sea-ice drift in the Central Arctic combining QuikSCAT and SSM/I sea ice drift data. User's Manual, Version 2.0, February 2007b.
ftp://ftp.ifremer.fr/ifremer/cersat/products/gridded/psi-drift/documentation/merged.pdf

Ezraty R., F. Girard-Ardhuin and D. Croizé-Fillon, Sea-ice drift in the Central Arctic using the 89 GHz brightness temperatures of the Advanced Microwave Scanning Radiometer. User's manual, Version 2.0, February 2007c.
ftp://ftp.ifremer.fr/ifremer/cersat/products/gridded/psi-drift/documentation/amsr.pdf

Kaleschke, L., C. Lüpkes, T. Vihma, J. Haarpaintner, A. Bochert, J. Hartmann and G. Heygster, SSM/I Sea ice remote sensing for mesoscale ocean-atmosphere interaction analysis, *Canadian Journal of Remote Sensing*, Vol. 27, n° 5, pp. 526-537, 2001

Kaleschke, L., Fernerkundung des Meereises mit passiven und aktiven Mikrowellensensoren, Dissertation, Fachbereich 1 (Physik/Elektrotechnik), Universität Bremen, 2003
http://elib.suub.uni-bremen.de/publications/dissertations/E-Diss628_Kaleschke.pdf

Kern, S., L. Kaleschke and D.A. Clausi. , A Comparison of two 85 GHz SSM/I Ice Concentration Algorithms with AVHRR and ERS-SAR, *IEEE Trans. Geoscience Remote Sensing*, 41(10), pp. 2294-2306, 2003

Liu A.K. and D.J. Cavalieri, On sea ice drift from the wavelet analysis of the Defense Meteorological Satellite Program (DMSP) Special Sensor Microwave Imager (SSM/I) data. *Int. J. Remote Sensing*, Vol. 19, No. 7, pp. 1,415-1,423. 1998

Svendsen, E., Mätzler C., and Grenfell, T.C. (1987). A model for retrieving total sea ice concentration from a spaceborne dual-polarized passive microwave instrument operating near 90 GHz, *Int. Journal of Remote Sensing*, Vol. 8, No. 10, pp. 1479-1487.

Contact

The best source of information is CERSAT : *http://www.ifremer.fr/cersat/*

CERSAT - IFREMER
BP 70
29280 Plouzané, France
Phone (33) 2 98-22-46-91
Fax (33) 2 98-22-45-33

For more information on **CERSAT archiving and processing facility (FPAF)**, please contact :

fpaf@ifremer.fr

M^r Jean-François PIOLLE
Phone (33) 2 98-22-46-91
Fax (33) 2 98-22-45-33
Internet : jfpiolle@ifremer.fr

M^r Denis CROIZE-FILLON
Phone (33) 2 98-22-47-12
Fax (33) 2 98-22-45-33
Internet : denis.croize.fillon@ifremer.fr

For more information on **PSI grids and products**, please contact :

M^r Robert EZRATY
Phone (33) 2 98-22-42-99
Fax (33) 2 98-22-45-33
Internet : robert.ezraty@ifremer.fr

M^rs Fanny GIRARD-ARDHUIN
Phone (33) 2 98-22-45-54
Fax (33) 2 98-22-45-33
Internet : fanny.ardhuin@ifremer.fr

Annex

SSM/I unavailable & incomplete data files

unavailable (m : missing) / partial-coverage (c) files
Year 1991
1991/12/03 (c)
1991/12/04 (c)
1991/12/04 (c)
1991/12/04 (c)
1991/12/16 (c)
1991/12/24 (c)
1991/12/30 (c)
1991/12/31 (c)
Year 1992
1992/01/08 (c)
1992/01/13 (c)
1992/01/14 (c)
1992/02/02 (c)
1992/02/14 (c)
1992/02/14 (c)
1992/02/14 (c)
1992/02/14 (c)
1992/03/03 (c)
1992/04/09 (c)
1992/04/11 (c)
1992/04/29 (c)
1992/04/30 (c)
1992/05/27 (c)
1992/06/05 (c)
1992/06/06 (c)
1992/06/07 (c)
1992/06/08 (c)
1992/06/17 (c)
1992/06/18 (m)
1992/07/14 (c)
1992/07/16 (c)
1992/07/28 (c)
1992/08/05 (c)
1992/08/24 (c)
1992/09/03 (c)
1992/10/01 (c)
1992/10/30 (c)
1992/11/06 (c)
1992/11/10 (c)
1992/11/27 (c)
1992/12/07 (c)
1992/12/13 (c)
1992/12/22 (c)
1992/12/23 (c)
1992/12/30 (c)

1992/12/31 (c)
Year 1993
1993/01/03 (c)
1993/01/04 (m)
1993/01/05 (c)
1993/01/08 (c)
1993/01/17 (c)
1993/01/31 (c)
1993/02/27 (c)
1993/02/28 (c)
1993/03/01 (c)
1993/03/10 (c)
1993/03/11 (c)
1993/04/26 (c)
1993/05/27 (c)
1993/06/20 (c)
1993/06/24 (c)
1993/07/13 (c)
1993/07/18 (c)
1993/07/20 (c)
1993/08/20 (c)
1993/11/17 (c)
1993/12/09 (c)
1993/12/11 (c)
1993/12/16 (c)
1993/12/17 (c)
1993/12/18 (c)
1993/12/28 (c)
Year 1994
1994/01/01 (c)
1994/02/03 (c)
1994/02/13 (c)
1994/02/16 (c)
1994/02/17 (c)
1994/02/28 (c)
1994/03/29 (c)
1994/05/09 (c)
1994/05/25 (c)
1994/05/26 (c)
1994/06/07 (c)
1994/06/08 (c)
1994/06/17 (c)
1994/06/19 (c)
1994/06/23 (c)
1994/06/24 (c)
1994/06/28 (c)
1994/06/29 (c)
1994/07/02 (c)
1994/07/11 (c)
1994/07/20 (m)
1994/07/21 (c)
1994/07/22 (c)
1994/08/31 (c)
1994/11/01 (c)
1994/11/06 (c)
1994/11/11 (c)
1994/11/20 (m)

1994/11/21 (m)
1994/11/22 (c)
1994/12/09 (c)
1994/12/12 (c)
1994/12/13 (c)
1994/12/17 (c)
1994/12/19 (c)
1994/12/25 (c)
Year 1995
1995/01/14 (c)
1995/03/24 (c)
1995/04/25 (c)
1995/04/27 (c)
1995/05/01 (c)
1995/05/03 (c)
1995/05/05 (c)
1995/05/06 (c)
1995/06/13 (c)
1995/06/13 (c)
1995/06/14 (c)
1995/07/12 (c)
1995/07/19 (c)
1995/07/24 (c)
1995/07/25 (c)
1995/12/19 (c)
1995/12/20 (c)
Year 1996
1996/01/27 (c)
1996/01/30 (c)
1996/03/08 (c)
1996/03/18 (c)
1996/03/25 (c)
1996/04/04 (c)
1996/04/07 (c)
1996/04/08 (c)
1996/04/14 (c)
1996/04/21 (c)
1996/04/23 (c)
1996/04/26 (c)
1996/05/11 (c)
1996/05/29 (c)
1996/05/30 (c)
1996/05/31 (c)
1996/06/01 (c)
1996/06/04 (c)
1996/06/05 (c)
1996/06/06 (c)
1996/06/22 (c)
1996/07/09 (c)
1996/08/14 (c)
1996/08/17 (c)
1996/08/20 (c)
1996/10/16 (c)
1996/10/27 (c)
1996/11/02 (c)
1996/11/03 (c)
1996/11/21 (c)

1996/11/30 (c)
1996/12/01 (m)
1996/12/03 (c)
Year 1997
1997/01/31 (c)
1997/02/15 (c)
1997/03/31 (c)
1997/04/15 (c)
1997/05/20 (c)
1997/05/31 (c)
1997/09/13 (c)
Year 1998
1998/03/10 (c)
1998/03/11 (m)
1998/03/12 (c)
1998/10/12 (c)
Year 1999
1999/01/16 (c)
1999/01/26 (c)
1999/11/08 (c)
1999/11/09 (c)
1999/11/17 (c)
Year 2000
2000/04/15 (c)
2000/04/16 (c)
2000/04/17 (c)
2000/05/04 (c)
2000/12/01 (m)
2000/12/02 (c)
Year 2001
2001/07/14 (c)
2001/11/14 (c)
Year 2002
2002/04/25 (c)
Year 2004
2004/09/28 (c)
2004/10/10 (c)
2004/10/11 (c)
2004/10/12 (c)
2004/10/13 (c)
2004/10/14 (c)
2004/10/15 (c)
2004/10/16 (c)
2004/10/17 (c)
2004/10/18 (c)
2004/10/19 (c)
2004/10/20 (c)
2004/10/22 (c)
2004/10/24 (c)
2004/10/25 (c)
2004/10/27 (c)
2004/10/29 (c)
2004/10/31 (c)
2004/11/05 (c)
2004/12/17 (c)

Year 2005
2005/02/26 (c)
2005/08/24 (c)
2005/08/27 (c)
2005/11/23 (c)
2005/12/08 (c)
2005/12/09 (c)
Year 2006
2006/01/26 (c)
2006/02/02 (c)
2006/02/03 (c)
2006/02/18 (c)
2006/04/16 (c)
2006/06/22 (c)
2006/07/06 (c)
2006/07/22 (c)
2006/08/02 (c)
2006/08/15 (c)
2006/10/28 (c)
2006/10/29 (c)
2006/12/01 (c)
2006/12/30 (c)
2006/12/31 (m)

Table 1: : Unavailable and incomplete data files as of February 2nd 2007.